



AN INVESTIGATION INTO THE NUMERICAL  
UNCERTAINTY OF RESISTANCE MODEL TANKER  
17.500 DWT

D Purnamasari<sup>1</sup>, I K A P Utama<sup>2</sup>, I K Suastika<sup>2</sup>

<sup>1</sup>Department of Naval Architecture,  
Institut Teknologi Sepuluh Nopember, Surabaya, Indonesia

<sup>2</sup>Department of Naval Architecture,  
Institut Teknologi Sepuluh Nopember Surabaya  
Indonesian Hydrodynamics Laboratory

ABSTRACT

*Credibility in computational simulations requires concerted and determined efforts to improve the reliability of the estimation of numerical accuracy. An understanding of the sources of the uncertainty can provide guidance on how to reduce or manage uncertainty in the simulation. The numerical simulation calculation and the error analysis of tanker 17.500 DWT resistance and the flow field has been investigated by the ITTC standard. It concerns the resistance calculation at different speeds from 1.029 m/s to 1.543 m/s (corresponding to a variation of the Froude number from 0.134 to 0.211) and the effect of two turbulence models EASM and  $k-\omega$ -SST on the results. The wave elevation on the hull has been measured and plotted, the verification is based on the turbulence model, the grid quantity, and the interaction between the grid quality and the turbulence model, Richardson extrapolations, and uncertainty analysis with factor of safety methods.*

**Keywords :** *resistance, verification, Richardson extrapolations, factor of safety, uncertainty analysis*

1.0 INTRODUCTION

Over the past few years there has been a growing interest in CFD techniques applied to ship hydrodynamics. Stern et al. (2013) reviewed the progress made over the last 10 years in CFD applied to ship hydrodynamics. Developments have led to CFD simulations being commonly integrated into the design process for new vessels. Larsson et al. (2013) added set of data resistance, sinkage and trim against Froude number for KVLCC2, KCS and DTMB useful for future validation of CFD results and to estimate the uncertainty in the data from the different facilities of 33 groups and 18 cases in the Gothenburg 2010 Workshop on Numerical Hydrodynamics. Credibility in computational simulations requires concerted and determined efforts to improve the reliability of the estimation of numerical accuracy. An understanding of the sources of the uncertainty can provide guidance on how to reduce or manage uncertainty in the simulation. Yao et al (2013) discussed the definition, the sources, the classification and the expressions of the CFD uncertainty.

---

\*Corresponding author: [limdh@fkm.utm.my](mailto:limdh@fkm.utm.my)

During the last fifteen years, much progress has been made in the development of robust and accurate computational strategies able to simulation of the water flow around ships. Free surface phenomenon around a ship hull plays an important role in its resistance, almost all methods used are based on the Navier-Stokes equations, the discretization methods for the water surface differ widely. Queutey and Visonneau (2007) built a new scheme for Blended Interface Capturing Scheme refined under the acronym for Blended Reconstructed Interface Capturing Scheme to keep constant the width of the interface on the smallest number of control volumes by reducing the numerical diffusion and dispersion, to ensure a monotonic change of the volume fraction. The ship resistance considering free surface presented by Pranzitelli et al (2011) was employed to simulate the free surface flow around a semi-displacing motor yacht hull. Shi et al (2012) ran many numerical simulations for the resistance of a ship model under different running attitudes and Froude numbers.

The current study aims to establish the resistance calculation and a numerical technique to simulate flow around the model hull of tanker 17.500 DWT at different speeds from 1.029 m/s to 1.543 m/s (corresponding to a variation of the Froude number from 0.134 to 0.211). This work describes the calculation of resistance force at steady forward speed with a free surface simulation using Volume-Of-Fluid (VOF) formulation. Multi-phase analyses have been done in this study by using the interface capturing an approach that solves the RANSE equations on a predetermined grid which covers the entire domain, the multi-block grids and the effect of two turbulence model EASM and  $k-\omega$ -SST on the results are being used to obtain numerical results.

## 2.0 MODEL GEOMETRY

The geometry studied is a model scale of the tanker 17.500 DWT. The main particulars are given in Table 1. This hull has a bulbous bow and a large block coefficient ( $C_B$ ). The hull geometry is depicted in Figs. 1-2. Waterline and profile view is given in Fig. 2

Table 1. Main particulars of the tanker 17.500 DWT

Particulars	Ship	Model
Length between perpendiculars	149.500 m	5980 mm
Breadth	27.700 m	1108 mm
Draft	7.000 m	280 mm
Displacement volume	23.464 m <sup>3</sup>	0.150 m <sup>3</sup>
Wetted surface area	5307 m <sup>2</sup>	8.491 m <sup>2</sup>
Scale Ratio		1/25

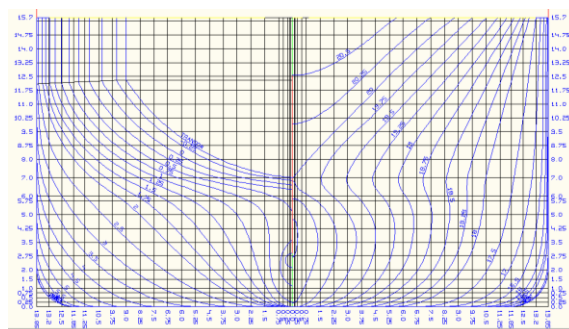


Figure 1. Body Plan of the tanker 17.500 DWT

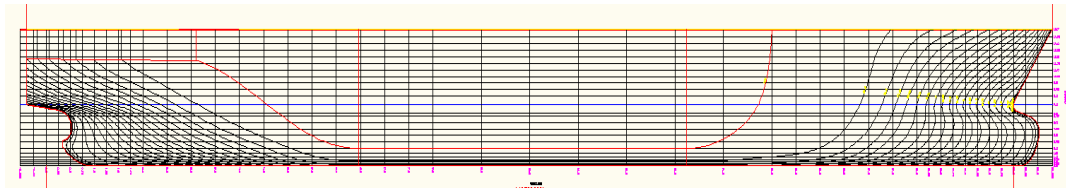


Figure 2. Waterlines of the tanker 17.500 DWT

### 3.0 NUMERICAL SETUP

The total resistance of a model scale hull was computed using CFD simulations based on the incompressible RANS equations, performed with the FINE/Marine flow solver. It included the unstructured Cartesian mesh using finite volume method formulation mesh generator HEXPRESS™, is aimed at the simulation of realistic flow problems in all branches of marine hydrodynamics (Numeca, 2013). A computational study based on the free-surface capturing approach to evaluate the flow field around hull in calm water.

A computational domain was created in the rectangular shape around the model and boundary condition shown graphically in Figure 3, dimensions from the model in terms of  $L_{pp}$ : Front  $1xL_{pp}$ , Back  $3xL_{pp}$ , Top  $1xL_{pp}$ , Bottom  $2xL_{pp}$ , Each side  $1.5xL_{pp}$ . The fluid flows along x-direction and positive y-axis points towards the starboard direction while z-axis points upward. A far field boundary condition was applied at the side, inlet and outlet boundaries. A slip wall condition was applied to the deck. A prescribed pressure boundary condition was applied to the top and bottom boundary.

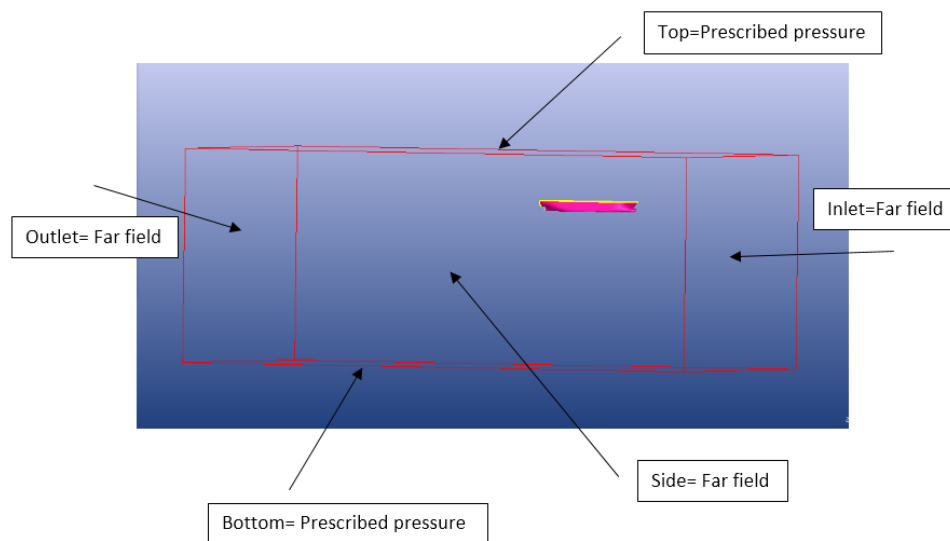


Figure 3. Representative domain boundaries

The grid was generated in five steps: initial mesh, adaptation to the geometry, snap to geometry, optimize mesh and viscous layer addition. Mesh generation to create unstructured hexahedral grids, an initial coarse grid which in the following is refined at the boundaries by subdividing initial cells. Then a mesh optimization was conducted to improve the quality of the cells. Finally, viscous layers were inserted on designated boundaries, see Numeca (2013). Figure 4 shows refinement around the geometry features and around the free surface.

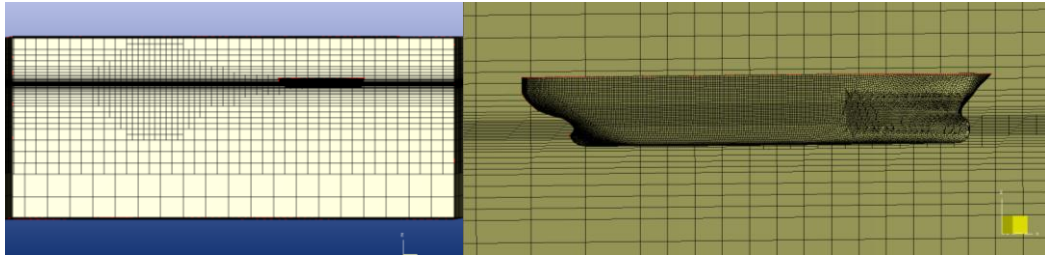


Figure 4. Generated unstructured full-hexahedral mesh

$K-\omega$  SST and EASM turbulence models were used with standard wall functions to model the Reynolds stress term, ITTC guidelines (ITTC 2011) recommend placing the first grid point at a distance from the ship's wall such that  $30 < y^+ < 100$ .

Table 2 shows to perform grid convergence analysis study based on changing the initial cell sizes, three volumic refinement boxes are added to the initial mesh resulting in three different meshes, with a cell count ranging from 1.4 million to 3.9 million., the different initial meshes will lead to different mesh sizes. This allows to refine the whole fluid volume and not only the areas right next to the solid.

Table 2. Number of cells for the mesh dependency study

	Initial mesh			Number of Cells
	x	y	z	
Coarse	10	6	4	1.487.007
Medium	15	9	6	2.513.477
Fine	20	12	8	3.942.362

Figure 5 (a.b.c) shows the complete generated mesh for coarse, medium and fine mesh respectively, approx 1.4 to 3.9 million cells for design speed  $Fr = 0, 175$ . The chosen wall distance for the generated meshes is  $y^+ = 30$ , so that a wall function implementation is used in the boundary conditions of the ship. Viscous prismatic cells around the hull consisted of 20 layers with an expansion ratio of 1.2.

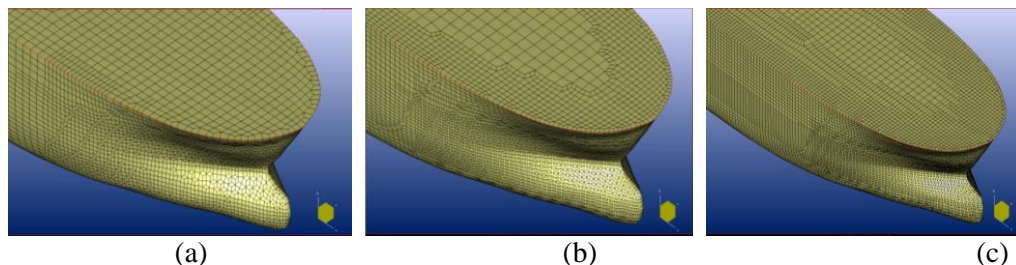


Figure 5 The complete generated mesh

The computational settings were common to time scheme: backward order, multi-fluid computation: water: dynamic viscosity:  $8.51(Pa.s) \times 10^{-4}$ , density:  $996.5kg/m^3$  and air: dynamic viscosity:  $1.85(Pa.s) \times 10^{-5}$ , density:  $1.2kg/m^3$ . Simulation control variables were as follows: 500 time steps, uniform time step = 50 sub-cycles, 8 non-linear iterations. The simulation was setup as a steady state solution, fixed in trim and heave to duplicate the conditions of the experimental data.

Convergence studies for grid spacing were undertaken to assess numerical errors for three solutions with refined mesh on the fine, medium, and coarse grids and uncertainties with grid sizes developed by Roache 1998. This method is currently used and recommended by ASME and the American Institute of Aeronautics and Astronautics (AIAA). Convergence studies of the 3 solutions to evaluate convergence with respect to

input parameter. Changes between the 3 solutions were used to define the convergence ratio:

$$R_i = \varepsilon_{i,21} / \varepsilon_{i,32} \quad (1)$$

Using generalized Richardson extrapolation, the order of accuracy  $r$ , the error in the solution  $\delta$ , and the uncertainty in the solution  $U$  can be estimated. For careful studies, the estimated error can be used to correct the solution and give corrected uncertainty  $U_c$ .

$$\delta_{RE_{i,1}}^{*(1)} = \frac{\varepsilon_{i,21}}{r_i^{p_i} - 1} \quad (2)$$

$$p_i = \frac{\ln(\varepsilon_{i,32} / \varepsilon_{i,21})}{\ln(r_i)} \quad (3)$$

A factor of safety approach was used to define the uncertainty where an error estimate from RE is multiplied by a factor of safety to bound simulation error followed the ITTC recommendation:

$$U_{ic} = (F_s - 1) |\delta_{RE_{i,1}}^*| \quad (4)$$

#### 4.0 RESULTS

Figure 6 shows typical solutions for a speed 1.338 m/s (Froude number of  $F_n=0.175$ ), distinct wave pattern develop, as well as a significant bow wave and the wave-length is larger than the length of the ship.

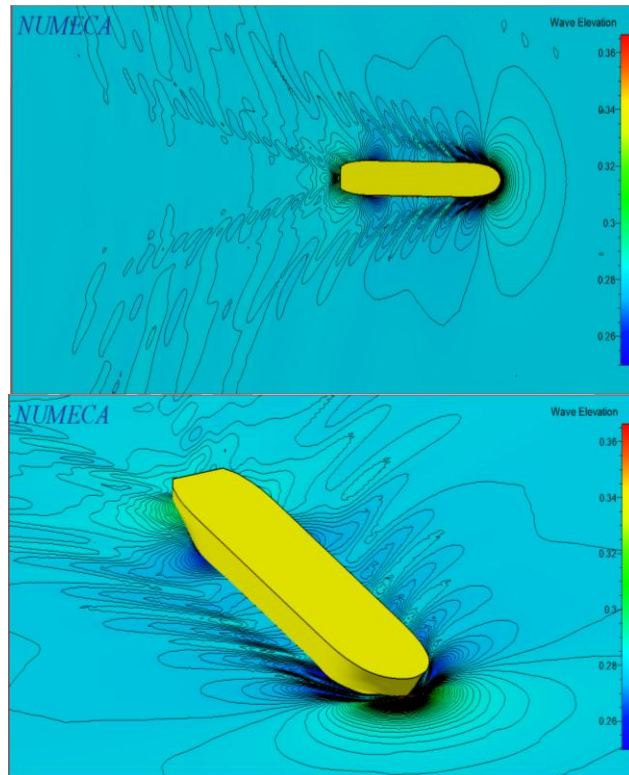


Figure 6. Wave elevation

The wave elevation on the hull has been measured and plotted, along a section situated at  $y/L_{pp}=0.148$ . Results are compared the calculation with the EASM model instead of the  $k\omega$ -SST.

The charts below compare wave elevation along X obtained with different turbulence model. Both models give exactly the same results.

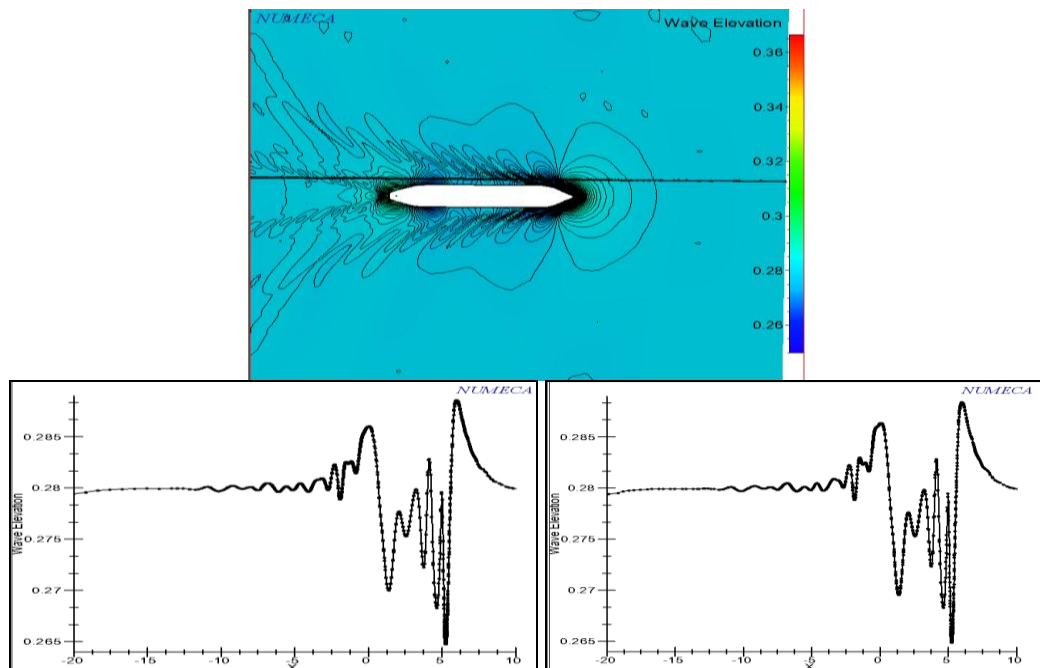
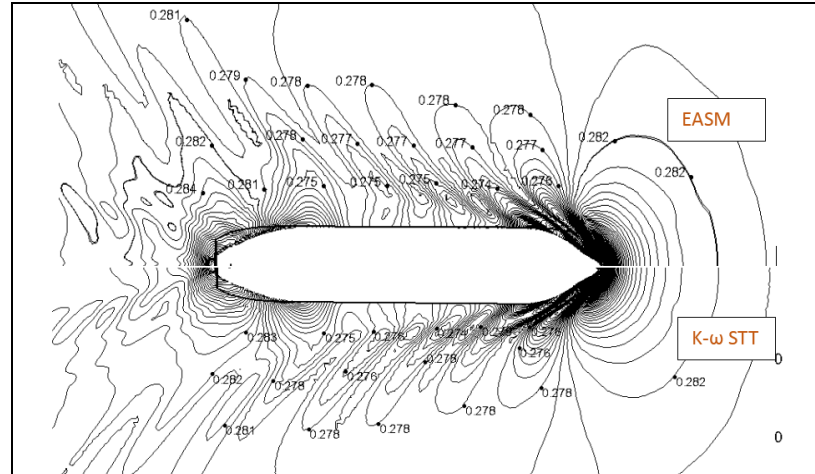


Figure 7. Wave elevation at  $y/L_{pp}=0.148$

The result of the isolines and local value were obtained from two turbulence model EASM and K- $\omega$ -SST, the free surfaces are match perfectly and quite the same.



Figures 9.

The contour plots of hydrodynamic pressure acting on the hull surface qualitatively coloured with the velocity magnitude. The effect of the hull wave pattern on the hull pressure distribution at the draft region was detected well by Fine Marine, the pressure increases again aft of the bow region due to the effect of hull geometry on the flow pattern around the hull at speed 1.338 m/s. Downstream of this position the pressure again decreases, and approximately extends over the entire region of the hull mid part due to nearly the constant cross-section of the hull in this region.

A graphical representation of the  $y^+$  for wall functions on the model hull, the first point from the wall is well within the logarithmic layer of the boundary layer, therefore value 30 is recommended ITTC 7.5-03 -02-03.

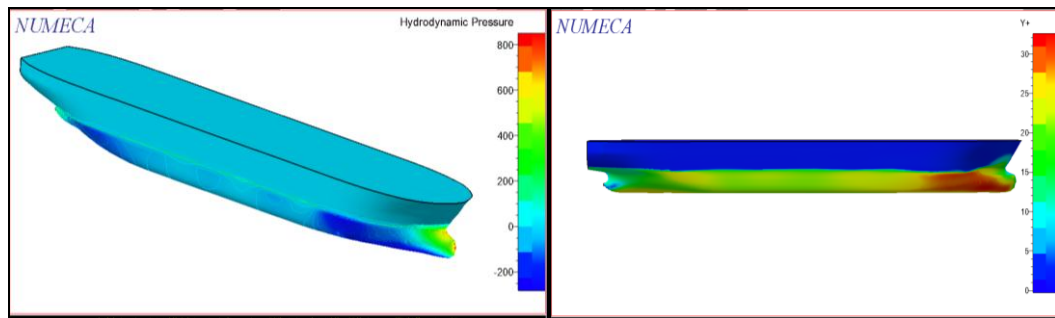


Figure 8. Hydrodynamic pressure (a) Wall  $Y^+$  distribution on the hull surface (b)

Table 3. Grid convergence study for total  $CT$  ( $10^3$ )

Froude number	Coarse	Medium	Fine	Experiment
0.134	4.56	4.42	4.15	4.21
0.148	4.61	4.51	4.12	4.23
0.161	4.59	4.49	4.12	4.29
0.175	4.71	4.57	4.15	4.35
0.188	3.69	3.78	3.99	4.25
0.201	4.21	4.37	4.96	4.59

Table 4. V&V result

$R$	$P$	$U_G$	$U_{SN}$	$U_{val}$
0.59	2.6	3.1%	1.1%	2.8%
0.68	3.4	2.6%	0.9%	2.1%
0.74	4.1	3.2%	1.5%	2.2%
0.60	3.8	2.9%	1.3%	2.6%
0.52	5.3	4.9%	1.9%	3.6%
0.64	4.3	3.8%	1.3%	2.9%

Table 3 shows the numerical results obtained from the three meshes, it indicates that the fine mesh predicts the total resistance with the highest accuracy. V&V results are shown in Table 4. It should be noted that the convergence condition corresponding to the 3 solutions shows as the monotonic convergence is achieved with the value  $R < 1$ . Every three grids adopted the same refinement ratio  $r_G = \sqrt{2}$ .

Figure 10 shows comparisons for total resistance coefficient  $C_T$ . EFD stands for Experimental Fluid Dynamics (experimental data), while CFD denotes the simulation results. It can be seen that numerical uncertainty is fairly minor based on the FS method, generally reduces for low Froude numbers but at larger Froude numbers they are slightly higher than the data uncertainty. Such a trend is expected as the boundary layer and free surface resolution of the grids is optimal for the design Froude number as mention above 13 knot, thus making the grids unsuitable for larger Froude numbers.

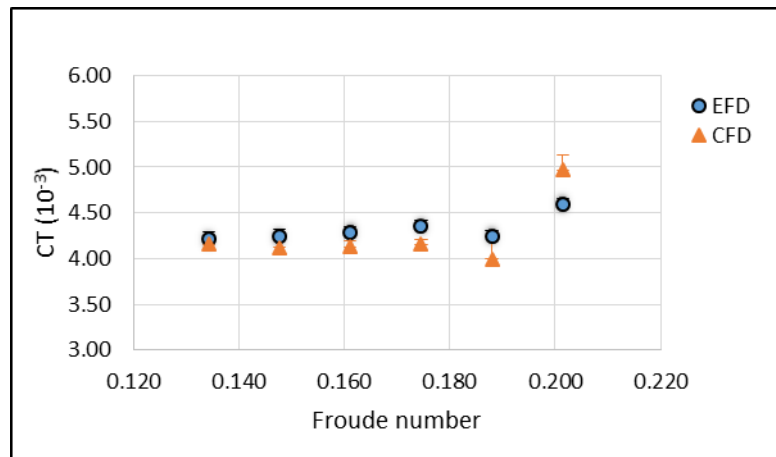


Figure 10. Total resistance coefficient

## 5.0 CONCLUSION

The excellent agreement between the model tests and CFD predictions for the total ship resistance in calm water condition results in a good confidence level in the CFD results presented. By using of turbulence models and wall functions resulted in wide variation to the final prediction. Mesh fineness requires being compatible with the turbulence model/wall functions being used to obtain meaningful results. The mesh quality has proven to be an important issue in the computations.

User skill and experience are important in making proper engineering judgment based on the simulation results of such a complicated problem as the free surface flow around the ship's hulls.

Future plans focus on the comparison of these simulation results using different RANSE methods, with the results of practical measurements.

## ACKNOWLEDGEMENTS

The first author, in particular, expressed her gratitude to The Ministry of Research and Technology (Ristekdikti) which funding her PhD program at ITS under contract number 07/S3/D/PTB/XI/2015 The authors would like to thank members of staff at Indonesian Hydrodynamic Laboratory for their sincere support during the experiment and manufacture of the ship model.

## REFERENCES

1. FINE™/Marine v3 Flow Integrated Environment for Marine Hydrodynamics. Documentation v3.1a, 2013
2. F.R.Menter. Two-Equation Eddy-Viscosity Turbulence Models for Engineering Applications. AIAA Journal. 32(8). 1598-1605. August 1994.
3. ITTC Recommended Procedures and Guide-lines. Uncertainty Analysis in CFD Verification and Validation. Methodology and Procedures, No. 7.5-03-01-01 (2008).
4. Larsson, L. Stern, F. Visonneau, M. 2014.Numerical Ship Hydrodynamics: An Assessment of the Gothenburg 2010 Workshop. Springer Verlag, Germany. Chapter 5.
5. L. Stern, S. Bhushan, T. Xing, M. Visonneau · J. Wackers · G. Deng, L. Larsson 2014.Numerical Ship Hydrodynamics: An Assessment of the Gothenburg 2010 Workshop. Springer Verlag, Germany. Chapter 7.

6. Numeca (2013). User Manual Hexpress.
7. Pranzitelli A, C de Nicola, S. Miranda, 2012, Steady State of Free Surface Flow Around Ship Hulls and Resistance Predictions, IX HMVS Naples, 25-27 May 2011
8. Queutey P and Visonneau M 2007 An interface capturing method for free-surface hydrodynamic flows *Computers & Fluids* 36(9) 1481–1510
9. Roache, P.J., 1998, *Verification and Validation in Computational Science and Engineering*, Hermosa publishers, Albuquerque, New Mexico.
10. Yao Zhen-qiu, SHEN Hong-cui, GAO Hui, 2013 A new methodology for the CFD uncertainty analysis, *Journal of Hydrodynamic* 25(1):131-147